

**OPTICAL AND X-RAY SPECTROSCOPY OF 1E 0449.4–1823:
DEMISE OF THE ORIGINAL TYPE 2 QSO**

Jules P. Halpern¹ and Michael Eracleous^{2,3}

Department of Astronomy, University of California, Berkeley, CA 94720

jules@astro.columbia.edu

and

Karl Forster

Department of Astronomy, Columbia University, 550 West 120th Street, New York, NY

10027

To appear in the *Astrophysical Journal*

July 1, 1998, Vol. 501

Received 9 September 1997; accepted 4 February 1998

¹Permanent address: Department of Astronomy, Columbia University, 550 West 120th Street, New York, NY 10027.

²Visiting Astronomer, Cerro-Tololo International Observatory, National Optical Astronomy Observatories, which is operated by AURA, Inc., under a cooperative agreement with the National Science Foundation.

³Hubble Fellow.

ABSTRACT

New optical spectra of the original narrow-line quasar 1E 0449.4–1823 show that it now has broad emission lines of considerable strength, eliminating it as a “type 2 QSO” candidate. Although broad emission-line components were probably present weakly in 1981 and 1984, they have certainly increased in strength, and are accompanied by Balmer continuum emission that makes the spectrum bluer than it was previously. We suggest that the behavior of 1E 0449.4–1823 is the same as that of some Seyfert 1.8 and 1.9 galaxies, in which Goodrich attributed long-term variations of their broad Balmer lines to dynamical motions of obscuring material located in or around the broad-line region. The optical continuum and broad emission-line regions of 1E 0449.4–1823 may still be partly covered in our line of sight, which would explain its large forbidden-line equivalent widths and flat α_{ox} relative to other low-redshift QSOs. Also present are apparent absorption features in the broad Balmer lines and in Mg II, which may be related to the past obscuration and current emergence of the broad-line region. However, it is difficult to distinguish absorption from broad emission-line peaks that are displaced in velocity; we consider the latter a plausible competing interpretation of these peculiar line profiles.

An *ASCA* X-ray spectrum of 1E 0449.4–1823 can be fitted with a power-law of $\Gamma = 1.63_{-0.09}^{+0.12}$, intrinsic $N_{\text{H}} < 9 \times 10^{20} \text{ cm}^{-2}$, and no Fe K α line emission. Its 2–10 keV luminosity is $6.7 \times 10^{44} \text{ ergs s}^{-1}$. Thus, there is no evidence for Seyfert 2 properties in the X-ray emission from 1E 0449.4–1823, which resembles that of an ordinary QSO. With regard to the still hypothetical type 2 QSOs, we argue that there is little evidence for the existence of *any* among X-ray selected samples.

Subject headings: galaxies: active – galaxies: Seyfert – galaxies: individual
(1E 0449.4–1823) – QSOs – X-rays: galaxies

1. Introduction

One basic fact about quasars is not yet understood, namely, why there are virtually no narrow-line or “type 2 QSOs,” the high-luminosity analogs of Seyfert 2 galaxies. Every year or so, an X-ray discovered object is advertised that might fit such a description, but its qualifications are usually found to be lacking for one reason or another. A handful of such cases were described in recent papers by Forster & Halpern (1996) and Halpern & Moran (1998), with generally negative evaluations. In this paper, we present new spectra of the “original” narrow-line QSO, the serendipitous X-ray source 1E 0449.4–1823 at $z = 0.338$ that was first to be described as such (Stocke et al. 1982). Although Stocke et al. referred to a possible broad component of $H\beta$ in their discovery paper, and even presented another spectrum (Stocke et al. 1983) showing a probable weak broad Mg II line in 1E 0449.4–1823 shortly after their original discovery, those observations have generally not been mentioned in subsequent discussions of this object. Instead, 1E 0449.4–1823 is invariably referred to as a Seyfert 2 galaxy or a narrow-line QSO without qualification (e.g., Stephens 1989; Miller & Goodrich 1990; Keel et al. 1994; Elizalde & Steiner 1995; Turner et al. 1997a, 1997b).

A weakness of the original studies of 1E 0449.4–1823 was their lack of coverage at $H\alpha$, which is sometimes the only broad emission line that is clearly detectable in X-ray selected Seyfert galaxies (e.g., Halpern, Helfand, & Moran 1995). Since this deficiency had not yet been remedied to our knowledge, we undertook to obtain spectra covering the Mg II, $H\beta$, and $H\alpha$ regions of 1E 0449.4–1823 in order to reassess its qualifications as a narrow-line QSO. We also reanalyzed an archival *ASCA* X-ray observation of 1E 0449.4–1823,

previously published by Turner et al. (1997a, 1997b), in the light of our new optical data. The observations and results of this investigation are reported below together with an interpretation of the broad-line components of substantial strength that we discovered in the optical spectrum. Possible implications of the dearth of type 2 QSOs in general are also discussed.

2. Optical Spectroscopy

Optical spectra of 1E 0449.4–1823 were obtained using the Kast spectrograph (Miller & Stone 1987) on the 3m Shane reflector of Lick Observatory, and on the CTIO 1.5m telescope. A log of the observations is given in Table 1. The spectrograph slit was oriented at the parallactic angle in order to ensure spectrophotometric accuracy. A composite of the spectra is shown in Figure 1, after standard reduction and dereddening by the extinction in this direction, which is estimated to be $E(B - V) = 0.078$ from the neutral hydrogen column density of Stark et al. (1992). We measure a heliocentric redshift of 0.3387 ± 0.0001 from the narrow emission lines, which is consistent with the systemic galaxy redshift that can be measured from the starlight that is definitely visible in the form of the Ca II K $\lambda 3933$ absorption line.

TABLE 1

Log of Optical Spectroscopy of 1E 0449.4–1823

Date (UT)	Telescope/Instrument	Exposure (s)	Wavelength (Å)	Resolution (Å)	Slit width (")
1996 Oct 11	Lick 3m/Kast Spec.	2×2400	3180–4526	4	2.0
1996 Oct 11	Lick 3m/Kast Spec.	2×2400	4697–7468	5	2.0
1997 Jan 5	CTIO 1.5m/RC Spec.	3×1500	7364–9152	3	1.8

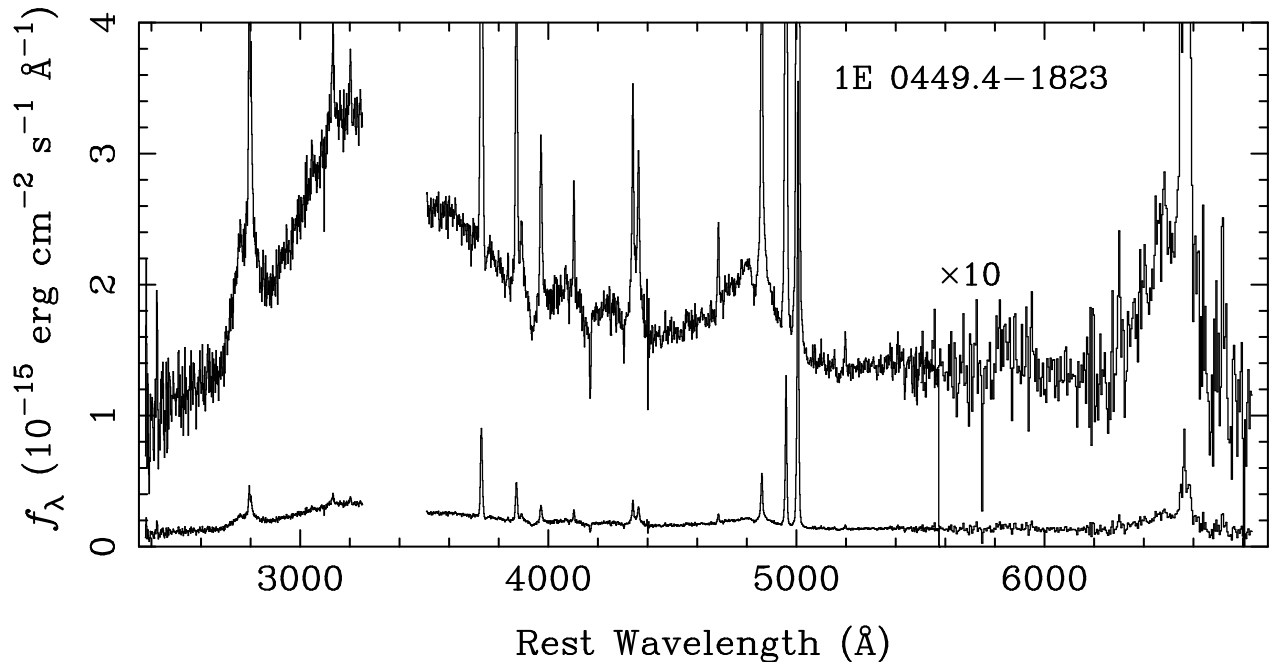


Fig. 1.— Combined spectra of 1E 0449.4–1823 from the Lick 3 m ($< 5500 \text{ \AA}$) and CTIO 1.5m ($> 5500 \text{ \AA}$). The flux scale refers to the lower trace. The upper trace is the same data multiplied by a factor of 10. The gap in the spectrum is due to our choice of dichroic filter for the Kast double spectrograph.

Immediately apparent in Figure 1 are broad emission lines of substantial strength, including Mg II, H β , and H α . The broad H β line, which here has rest EW = 55 \AA , was not obvious in the spectra of Stocke et al. (1982) obtained in 1981, and that of Stephens (1989) obtained in 1984. However, the former authors noted its possible presence, and it can be seen weakly upon close inspection of the spectrum of the latter. In addition to the improved signal-to-noise ratio here, the broad lines have definitely increased in strength since the early 1980s. Another factor that hindered the previous detection and measurement of the broad emission lines is their large velocity width, $\approx 10,000 \text{ km s}^{-1}$ FWHM and $\approx 20,000 \text{ km s}^{-1}$ FWZI. In fact, this large velocity width is still a significant factor limiting the accuracy to which the Balmer lines can be measured; it is difficult to define a continuum blueward of

$H\beta$ because of blending with the higher-order Balmer lines. Accompanying those lines are an increase in the Balmer continuum which is responsible for the broad bump in the near ultraviolet. This “little blue bump” was not present in the previous spectra, leading Stocke et al. (1982) to describe 1E 0449.4–1823 as a red object, with $U - B = -0.4$. Although the *rest frame* $U - B$ color is now -0.8 as estimated from our spectrum, there is probably still significant reddening of the continuum as indicated by its steepness in the neighborhood of the Mg II line. In contrast, Grandi & Phillips (1979) show spectra of QSOs that are rising shortward of the Mg II line.

Line intensity measurements for both broad and narrow components are given in Table 2. There is not much evidence for reddening in the emission-line spectrum. Both the narrow-line and broad-line Balmer decrements are consistent with those of unreddened QSOs. The broad Mg II/ $H\beta$ ratio is 0.85, within the range 0.5–2.5 that is usually found in QSOs (Grandi & Phillips 1979), and similar to those of other X-ray selected AGNs (Puchnarewicz et al. 1997).

There is one noteworthy property of the spectrum of 1E 0449.4–1823. A close examination of the broad emission lines shows that their profiles (Figure 2) all have the same unusual structure, which can be described either as an absorption feature blueshifted by -1900 km s^{-1} from the galaxy rest frame, or else as a well-defined broad emission-line peak blueshifted by -3500 km s^{-1} . Although narrow absorption lines such as these are common in the resonance lines of Seyfert galaxies, they are virtually unknown in the Balmer lines, which makes us reluctant to adopt the absorption-line hypothesis. Alternatively, displaced broad emission-line peaks are common in Balmer lines and Mg II, but those are usually found in radio galaxies or Seyferts of moderately high radio luminosity (Eracleous & Halpern 1994), whereas 1E 0449.4–1823 is radio quiet, with flux densities of 1.1 mJy at 6 cm (Feigelson, Maccacaro, & Zamorani 1982) and 3.3 mJy at 20 cm (Condon et al.

1996, the NRAO VLA Sky Survey). [Although Ellsington, Yee, & Green (1991) refer to 1E 0449.4–1823 as radio loud, this is clearly not the case, as its monochromatic power at 20 cm is only 2.2×10^{24} W Hz⁻¹. Throughout this paper we use $H_0 = 50$ km s⁻¹ Mpc⁻¹ and $q_0 = 0$.]

One reason that it is difficult to decide between these two descriptions of the spectra (absorption vs. displaced emission) is that the contaminating narrow-line components are so strong. Even better spectra would be needed to distinguish between these hypotheses.

TABLE 2
Emission-Line Measurements of 1E 0449.4–1823

Line Identification	Flux ^a	Intensity ^b	FWHM	EW ^c
	$F/F(\text{H}\beta)$	$I/I(\text{H}\beta)$	(km s ⁻¹)	(Å)
Mg II λ 2795[narrow]	0.32	0.37	...	6
Mg II λ 2802[narrow]	0.17	0.20	...	2
Mg II λ 2798[broad]	1.75	2.04	10,200	47
[O III] λ 3132	0.21	0.24
He II λ 3203	0.10	0.11
[O II] λ 3727	1.61	1.73	...	27
[Ne III] λ 3869	0.72	0.77
He I λ 3888, H ζ	0.29	0.31
[Ne III] λ 3968, H ϵ	0.46	0.48
H δ [n]	0.35	0.36
H γ [n]	0.43	0.44
H γ [b]	0.86	0.89	9,200	21
[O III] λ 4363	0.48	0.49

TABLE 2 (cont.)

Line Identification	Flux ^a	Intensity ^b	FWHM	EW ^c
	$F/F(\text{H}\beta)$	$I/I(\text{H}\beta)$	(km s ⁻¹)	(Å)
He II λ 4686	0.15	0.15
H β [n]	1.00	1.00	...	27
H β [b]	2.41	2.41	10,900	55
[O III] λ 4959	2.43	2.42	...	67
[O III] λ 5007	7.22	7.17	...	195
[N I] λ 5199	0.07	0.06
[O I] λ 6300	0.44	0.42
[N II] λ 6548	0.56	0.52	...	19
H α [n]	2.63	2.46	...	87
H α [b]	10.16	9.53	9,470	285
[N II] λ 6583	1.12	1.05	...	37
[S II] λ 6716	0.54	0.50
[S II] λ 6731	0.24	0.22

^aObserved flux relative to $F(\text{H}\beta[n]) = 3.13 \times 10^{-15}$ ergs cm⁻² s⁻¹.

^bIntensity corrected for Galactic $E(B - V) = 0.078$ mag, relative to $I(\text{H}\beta[n]) = 3.75 \times 10^{-15}$ ergs cm⁻² s⁻¹.

^cRest frame equivalent width.

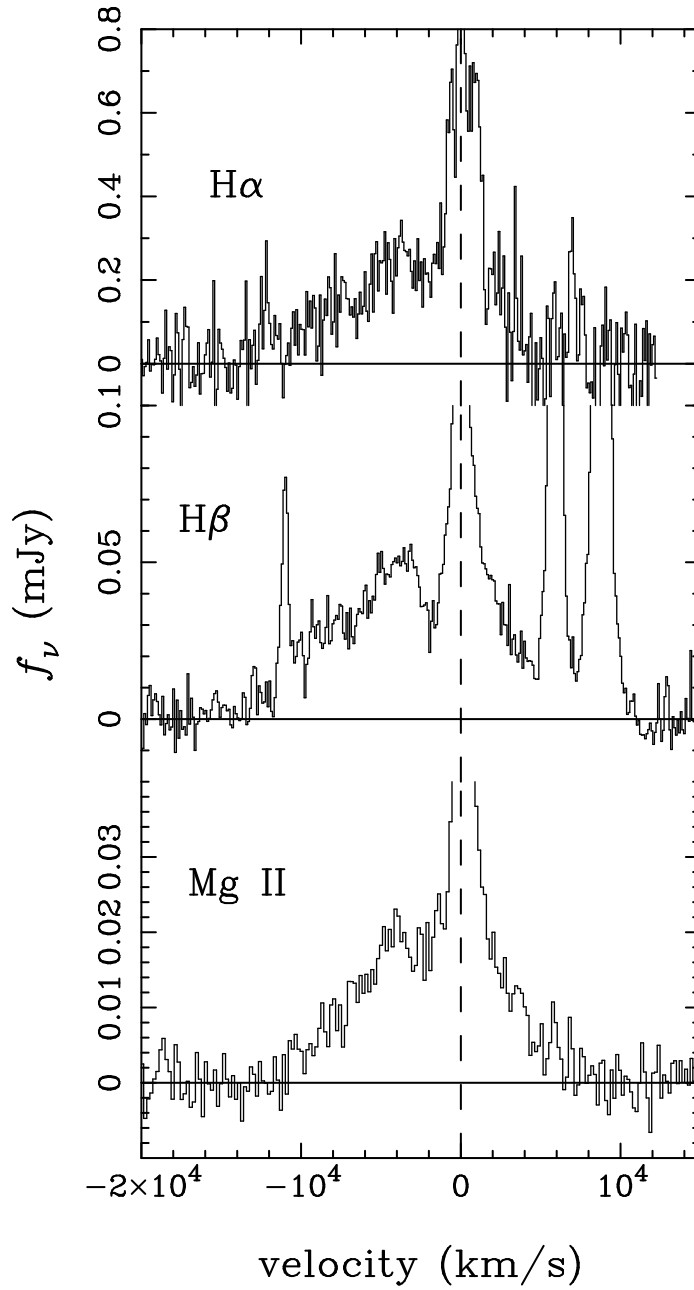


Fig. 2.— Continuum subtracted spectra of the broad emission lines of 1E 0449.4–1823 in velocity units. Structure in the broad emission lines can be described either as absorption centered at -1900 km s $^{-1}$, or a displaced broad emission-line peak at -3500 km s $^{-1}$.

3. ASCA X-ray Observation

1E 0449.4–1823 was observed by the *ASCA* satellite on 1994 March 4–5. Data obtained with the four instruments on board *ASCA* were obtained from the archive, and were filtered following the standard procedures described in *The ABC Guide to ASCA Data Reduction*. The SIS detectors were operated in 2-CCD mode, with the target placed at the default 1-CCD position. Source counts in the SIS images were extracted using a 3' radius circular region, and background counts were collected from the entire chip, excluding a 4' radius region centered on the target. In the GIS images, source counts were extracted using a region 6' in radius. The GIS background was measured in a source-free part of the image located the same distance off-axis as 1E 0449.4–1823 with an area equal to that used to extract the target. Useful exposure times and average background-subtracted source count rates in the four *ASCA* detectors are listed in Table 3.

TABLE 3

<i>ASCA</i> Observation Summary		
	Exposure Time	Count Rate, 0.5–10 keV
Instrument	(s)	(counts s ⁻¹)
SIS0	33,110	3.56×10^{-2}
SIS1	32,627	2.38×10^{-2}
GIS2	36,669	2.06×10^{-2}
GIS3	36,667	2.58×10^{-2}

For spectral fitting, the SIS and GIS spectra were rebinned to have at least 20 counts (source plus background) per channel. All four detectors were modelled simultaneously, but for clarity of presentation, the summed SIS and summed GIS spectra are shown in Figure 3. The spectra are modelled with a power law absorbed by a column of neutral gas

fixed at the Galactic value ($3.88 \times 10^{20} \text{ cm}^{-2}$; Stark et al. 1992). A second absorption component was included as a free parameter at the redshift of 1E 0449.4–1823. It was found that this additional intrinsic column did not improve the fit and only an upper limit of $N_{\text{H}}^{\text{Int}} < 8.8 \times 10^{20} \text{ cm}^{-2}$ (90% confidence) can be derived (see Figure 4). The photon index is found to be $\Gamma = 1.63_{-0.09}^{+0.12}$ and the observed flux between 0.5 and 10 keV is $1.6 \times 10^{-12} \text{ ergs cm}^{-2} \text{ s}^{-1} \text{ keV}^{-1}$ (the average of the four instruments). The intrinsic luminosity of 1E 0449.4–1823 in the rest frame 2–10 keV band is $6.7 \times 10^{44} \text{ ergs s}^{-1}$.

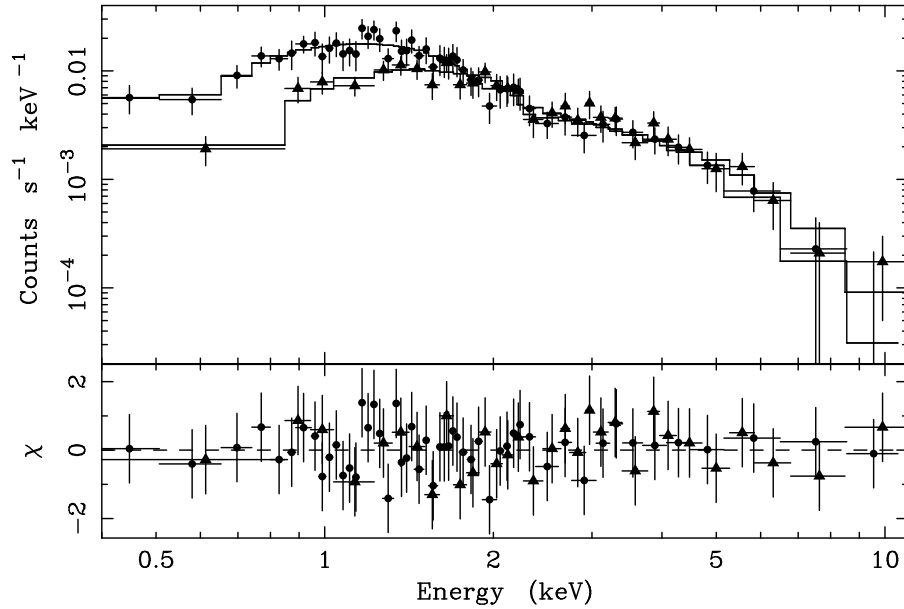


Fig. 3.— The observed *ASCA* SIS (filled circles) and GIS (filled triangles) spectra of 1E 0449.4–1823 and best fitting power-law of $\Gamma = 1.63$, absorbed by the Galactic column of $3.9 \times 10^{20} \text{ cm}^{-2}$. The model is a simultaneous fit to all four instruments separately, while the figure shows the summed SIS and GIS data for clarity.

No emission or absorption features are evident in the residuals from the power-law fit; the upper limit to the equivalent width of a narrow Fe $K\alpha$ emission line at rest frame energy 6.4 keV is $< 440 \text{ eV}$. The model fit is not improved significantly by the addition

TABLE 4

Power-Law Fit to the *ASCA* Spectra of 1E 0449.4–1823

Energy Range	N_{H}^{a}			Flux	
(keV)	Γ	(10^{20} cm^{-2})	A^{b}	χ^2 (d.o.f.)	($\text{ergs cm}^{-2} \text{ s}^{-1}$)
0.5–10	$1.63_{-0.09}^{+0.12}$	< 8.8	2.45	168.3 (212)	1.6×10^{-12}

^aColumn density intrinsic to 1E 0449.4–1823, in addition to the Galactic column of $3.9 \times 10^{20} \text{ cm}^{-2}$.

^bPower-law normalization at 1 keV in the observed frame, in units of $10^{-4} \text{ photons cm}^{-2} \text{ s}^{-1} \text{ keV}^{-1}$ (average of the four instruments).

of such a line ($\Delta\chi^2 = 0.01$). In this respect, 1E 0449.4–1823 differs from the Seyfert 2 galaxies like NGC 1068, NGC 4945, and NGC 6552 that have fluorescent Fe K α lines of $EW = 1.0 - 1.5 \text{ keV}$ (Marshall et al 1993; Iwasawa et al. 1993; Reynolds et al. 1994). Instead, it is more similar to Seyfert 1 galaxies or QSOs.

The *ASCA* X-ray spectrum of 1E 0449.4–1823 is entirely consistent with the luminosity measured by *Einstein* in the 0.3–3.5 keV band, $5.6 \times 10^{44} \text{ ergs s}^{-1}$ (Maccacaro et al. 1991), and the UV continuum brightness has not increased either since the observation of Stocke et al. (1983). Therefore, we have not even indirect evidence that the growth of the broad emission lines that we observe in the optical spectrum was caused by an increase in the intrinsic ionizing luminosity of the nucleus. However, the nonsimultaneity of the X-ray and optical observations, and the lack of regular monitoring during the 15 years since the *Einstein* discovery, make this inference about the absence of causation an unreliable one. Nevertheless, we offer an alternative explanation for the emergence of the broad emission lines in §4.

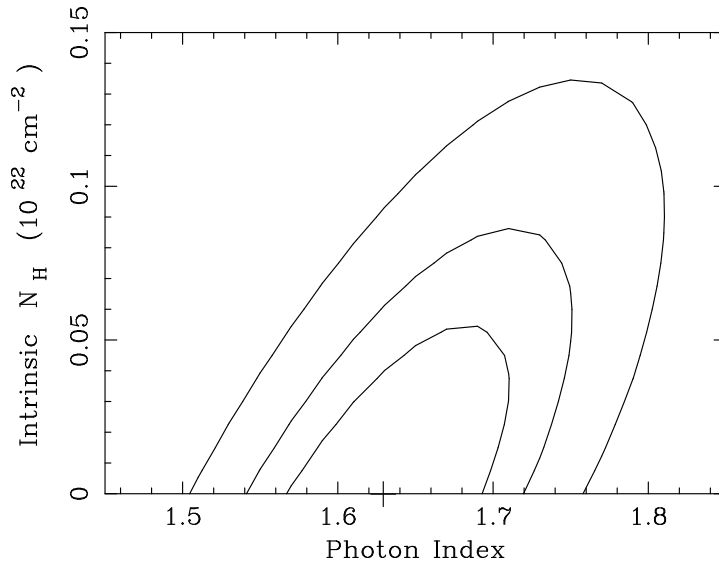


Fig. 4.— Confidence contours for the parameters of the power-law model fitted simultaneously to the SIS and GIS spectra of 1E 0449.4–1823. Contours represent the 68%, 90%, and 99% confidence limits for two interesting parameters. Only an upper limit to the intrinsic column density can be measured, while treating the Galactic column of $3.9 \times 10^{20} \text{ cm}^{-2}$ as a fixed parameter.

We calculate the X-ray to optical slope α_{ox} , defined as $-\log(f_x/f_o) / \log(\nu_x/\nu_o)$, where the flux densities f_x and f_o are calculated at frequencies ν_x and ν_o corresponding to 2 keV and 2500 Å, respectively, in the rest frame. The result is $\alpha_{ox} = 0.93$, smaller than the value of 1.15 quoted by Stocke et al. (1982), perhaps as a result of our more accurate measurement of the continuum at 2500 Å. This value is unusually small for radio-quiet quasars, implying either a deficit of UV emission or an X-ray excess. Typical values are in the range 1.1–1.7 (Stocke et al. 1990; Boroson & Green 1992), indicating, for example, that 1E 0449.4–1823 could be underluminous in the UV by a factor of 4 or more.

4. Discussion

4.1. So, what is 1E 0449.4–1823 anyway?

With the discovery of a normal complement of broad emission lines, there is no longer much to distinguish 1E 0449.4–1823 from an ordinary, low-luminosity QSO. Its absolute magnitude $M_V = -23.5$ meets the QSO criteria, and the equivalent widths of its broad lines as listed in Table 2 are also in the normal range. For example, its broad Mg II equivalent width of 47 Å is comparable to the average value of 67 Å found by Francis, Hooper, & Impey (1993), 64 Å found by Zheng et al. (1997), or 34 Å found by Steidel and Sargent (1991), for radio-quiet quasars in general, and is similar to many of the individual objects in Corbin & Boroson (1996). The X-ray luminosity of 1E 0449.4–1823 in the intrinsic 2–10 keV band is 6.7×10^{44} ergs s⁻¹, which is also typical of low-luminosity QSOs. The upper limit of 9×10^{20} cm⁻² on any intrinsic column density obscuring the X-ray spectrum allows for little equivalent visual extinction, $E(B - V) < 0.18$. Furthermore, there is nothing unusual about the *ratio* of X-ray (2–10 keV) to broad H α flux, which is ≈ 30 , very close to the mean value of 40 found for a large sample of Seyfert 1 galaxies by Elvis, Soltan, & Keel (1984). Similarly, the ratio of X-ray to [O III] luminosity of 1E 0449.4–1823 is similar to that of Seyfert 1 and Seyfert 2 galaxies as shown in Figure 5, adapted from Mulchaey et al. (1994). However, the large equivalent widths of its *narrow* emission lines are somewhat unusual. In Figure 6, we compare several properties of 1E 0449.4–1823 with those of the 87 low-redshift quasars in the PG sample (Boroson & Green 1992). 1E 0449.4–1823 stands out in its [O III] equivalent width, which is larger than that of all the PG quasars. Its FWHM of H β is also at the very high end of the distribution, though it would not be unusual among radio-loud quasars (Eracleous & Halpern 1994).

The original optical spectra from Stocke et al. (1982,1983) and Stephens (1989) appeared redder than ours, with no evidence for a blue bump, and broad lines that were

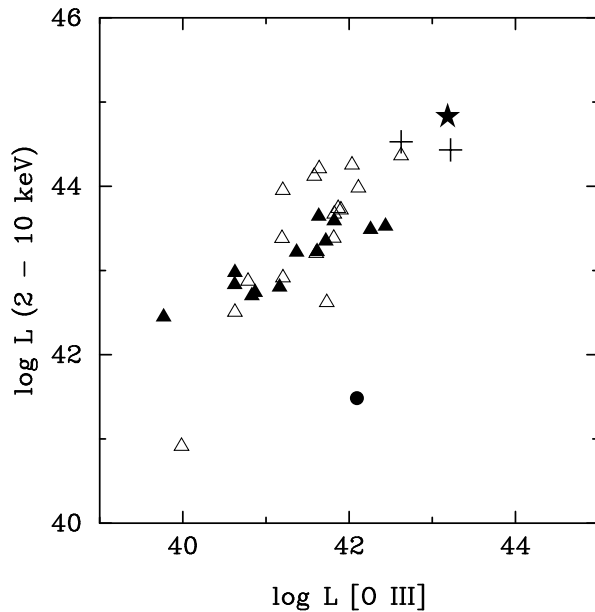


Fig. 5.— Properties of Seyfert galaxies and type 2 QSO candidates with hard X-ray spectra. Seyfert 1s (open triangles) and Seyfert 2s (filled triangles) are from Figure 3c of Mulchaey et al. (1994). The filled circle is NGC 1068. Crosses are the ultraluminous *IRAS* galaxies 23060+0505 and 20460+1925 from Brandt et al. (1997) and Ogasaka et al. (1997), respectively. The star is 1E 0449.4–1823.

weak at best. The long-term variability of the Balmer lines and Balmer continuum is obvious, although difficult to quantify because we do not have the historical spectra in digital form. In this respect, the behavior of 1E 0449.4–1823 resembles that of many Seyfert 1.8 and 1.9 galaxies, in which the broad Balmer-line components are highly variable on time scales of years. Goodrich (1989, 1995) has attributed this effect in at least some objects to partial obscuration in and around the broad-line region, which can vary on the dynamical time scale of the clouds containing the dust. The variability can be quite dramatic; some objects originally classified as intermediate Seyferts because of their barely detectable broad-line components appear years later as ordinary Seyfert 1 galaxies. Indeed,

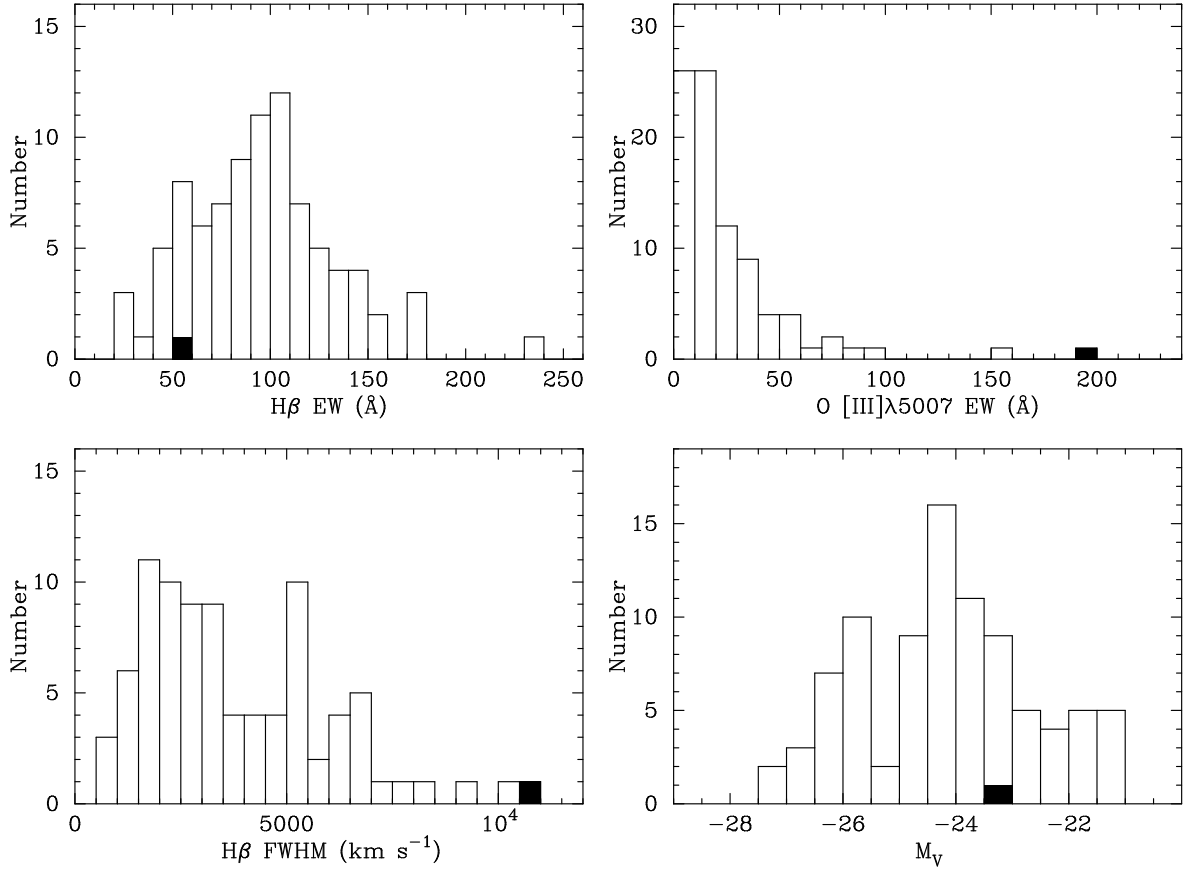


Fig. 6.— Comparison of the properties of 1E 0449.4–1823 (dark square) with those of the 87 low-redshift PG quasars from Boroson & Green (1992).

if most intermediate type Seyferts spend only a fraction of their time in a “low state,” then any deliberate survey for them will amass objects that will later change their classification to Seyfert 1. And if the probability of such variable obscuration declines with increasing luminosity, then this can explain why the rare “type 2 QSO” discovered among hundreds of X-ray sources is likely to revert eventually to an ordinary type 1 spectrum.

We propose, therefore, that 1E 0449.4–1823 is simply a higher luminosity example of these variable intermediate Seyfert galaxies. It is possible that part of the broad-line region of 1E 0449.4–1823 is still covered, which could account for the unusual shape of its

emission-line profiles. Furthermore, if the continuum emitting region is still partly obscured, which would be consistent with the fact that the V magnitude estimated from our spectrum has not changed significantly from the value of $V = 18.5$ measured by Stocke et al. (1992), then this partial obscuration might explain why the [O III] equivalent width is so large. It is likely that the [O III] luminosity represents the time-averaged photoionizing flux seen by the narrow-line region. If our present line of sight to the continuum is more obscured than the average one, while the narrow-line region is unobscured, then both the large equivalent width of [O III] and the relatively flat $\alpha_{ox} = 0.93$ could be accounted for by a depression of the observed UV/optical continuum by about a factor of 4. Turning now to the X-rays, since the observed X-ray luminosity has not changed significantly from the *Einstein* value, and in the absence of any evidence for partial covering or reflection in the X-ray spectrum, it is probably the case that our line of sight to the X-ray source is unimpeded, and that the observed X-ray luminosity is a fair representation of its intrinsic value.

An important test of these conclusions can be provided by spectropolarimetry. Most intermediate Seyfert galaxies are weakly polarized, but when they do show polarization it is often variable, with the continuum and emission lines having different position angles and wavelength dependence (Goodrich 1989,1995; Martel 1997). Such complex behavior, or a lack of polarization altogether, would be evidence for our hypothesis that we are getting a direct view of at least parts of the broad-line and continuum emitting regions. The alternative view of 1E 0449.4–1823 as type 2 QSO in unified schemes would predict uniform polarization across the broad emission lines and continuum, caused by electron scattering of the light from an otherwise hidden AGN, with possible dilution from a second, unpolarized continuum source. In that case, the broad-emission lines should be stronger in polarized light than in the direct flux spectrum, in exact analogy with the hidden Seyfert 1 galaxies (Miller & Goodrich 1990, Tran 1995). If it is a hidden QSO, 1E 0449.4–1823 would then be similar to the hidden Seyfert 1 galaxy Wasilewski 49 (Moran et al. 1992), which is

the only one of its class in which broad emission-line components are clearly visible in its direct flux spectrum. While we believe that the observed change in the broad emission lines of 1E 0449.4–1823 already argues against the hidden QSO model (e.g., the lines have *not* been seen to vary in Was 49), the value of independent confirmation via spectropolarimetry is evident.

4.2. Are there any Type 2 QSOs?

Having stricken 1E 0449.4–1823 from the short list of candidates that are occasionally nominated for the honor of type 2 QSO, it remains for us to ask if there are *any* such objects. That is, are there any high-luminosity counterparts of Seyfert 2 galaxies. Forster & Halpern (1996) and Halpern & Moran (1998) recently addressed this question with regard to the handful of such X-ray selected objects, offering a generally pessimistic evaluation of the qualifications of the proposed candidates, and eliminating all but one from active consideration. The reader is referred to those papers for detailed case histories. The only remaining X-ray selected candidate that is still claimed to be a type 2 QSO is a very faint emission-line object, the *ASCA* source AX J08494+4454 at $z = 0.9$ (Ohta et al. 1996). In view of its faintness, we consider this object to be no stronger a candidate than the others which have since been rejected. At time of this writing, there is a dearth of evidence for the existence of *any* type 2 QSO among X-ray selected AGNs.

Of course, in the standard unified scheme there are no *true* Seyfert 2 galaxies, only Seyfert 1s hidden by molecular tori. We repeat here the discussion of Halpern & Moran (1998) with regard to the possible implications. In the unified scheme, the absence of type 2 QSOs among X-ray selected samples is natural if either 1) the X-rays from all such objects are hidden from view, or 2) all sufficiently luminous QSO nuclei are able to remove any obscuring dust from their vicinity, allowing their broad-line regions to be visible from any direction. Although a number of ultraluminous *IRAS* galaxies have Seyfert 2 spectra

and hidden broad-line regions (e.g., Wills & Hines 1997, and references therein), there is not much evidence that they harbor *luminous* X-ray sources (e.g., Brandt et al. 1997; Ogasaka et al. 1997). The most luminous X-ray source in the nucleus of a ultraluminous *IRAS* galaxy is *IRAS* 23060+0505, but its 2–10 keV luminosity is only 1.5×10^{44} ergs s⁻¹ (Brandt et al. 1997), well within the range of Seyfert 1 galaxies as illustrated in Figure 5. While both of the explanations offered above may be responsible to some degree for the dearth of type 2 QSOs, there are counterexamples to either. First, a substantial number of Seyfert 2 galaxies *are* detected in hard X-rays because their column densities, in the range $10^{23} - 10^{24}$ cm⁻², are not so large as to be completely opaque (e.g., Awaki et al. 1991; Salvati et al. 1997). Second, even objects of modest quasar-like luminosity, principally radio galaxies like Cygnus A, are able to retain their obscuring material while permitting their broad Mg II emission lines to be visible in (Rayleigh) scattered light (Antonucci, Hurt, & Kinney 1994). A power-law nuclear X-ray source with 2–10 keV luminosity of $\sim 1 \times 10^{45}$ ergs s⁻¹ was detected in Cygnus A by *Ginga* (Ueno et al. 1994). So it seems that the obscuring gas and dust that is essential to the unified scheme is neither so substantial as to prevent direct X-ray detection or indirect UV scattering, nor so fragile as to be destroyed in the QSO environment. Thus, the absence of type 2 X-ray sources of higher luminosity, and the rarity of type 2 QSOs compared to ordinary QSOs, remain significant facts to be explained whether in the context of unified models or not. The two commonly offered explanations mentioned at the beginning of this paragraph, while having considerable promise, could both use additional detailed evaluation. In particular, identifications and careful spectroscopy of serendipitous sources in deep and *AXAF* surveys should provide the most sensitive test for hidden QSOs in hard X-rays. Moderate to high redshifts would aid in the detectability of highly absorbed sources by shifting their hard X-rays to lower energy. If no type 2 QSOs are found in these surveys, the simplest interpretation may be that they do not exist.

This work was supported by a grant from NASA under the *ASCA* Guest Investigator Program (NAG 5-2524). This paper is contribution 646 of the Columbia Astrophysics Laboratory.

REFERENCES

- Antonucci, R., Hurt, T., & Kinney, A. 1994, *Nature*, 371, 313
- Awaki, H., Koyama, K., Inoue, H., & Halpern, J. P. 1991, *PASJ*, 43, 1995
- Boroson, T. A., & Green, R. F. 1992, *ApJS*, 80, 109
- Brandt, W. N., Fabian, A. C., Takahashi, K., Fujimoto, R., Yamashita, A., Inoue, H., & Ogasaka, Y. 1997, *MNRAS*, 290, 617
- Condon, J. J., Cotton, W. D., Griesen, E. W., Yin, Q. F., Perley, R. A., Taylor, G. B., & Broderick, J. J. 1996, preprint
- Corbin, M. R., & Boroson, T. A. 1996, *ApJS*, 107, 69
- Ellsington, E., Yee, H. K. C., & Green, R. F. 1991, *ApJ*, 371, 49
- Elvis, M., Soltan, A., & Keel, W. C. 1984, *ApJ*, 283, 479
- Eracleous, M., & Halpern, J. P. 1994, *ApJS*, 90, 1
- Feigelson, E. D., Maccacaro, T., & Zamorani, G. 1982, *ApJ*, 255, 392
- Forster, K., & Halpern, J. P. 1996, *ApJ*, 468, 565
- Francis, P. J., Hooper, E. J., & Impey, C. D. 1993, *AJ*, 106, 417
- Goodrich, R. W. 1989, *ApJ*, 340, 190
- . 1995, *ApJ*, 440, 141
- Grandi, S. A., & Phillips, M. M. 1979, *ApJ*, 232, 659
- Halpern, J. P., Helfand, D. J., & Moran, E. C. 1995, *ApJ*, 453, 611

- Halpern, J. P., & Moran, E. C. 1998, *ApJ*, 494, 000
- Iwasawa, K., Koyama, K., Awaki, H., Kunieda, H., Makishima, K., Tsuru, T., Ohashi, T.,
& Nakai, N. 1993, *ApJ*, 409, 155
- Keel, W. C., De Grijp, M. H. K., Miley, G. K., & Zheng, W. 1994, *A&A*, 283, 791
- Maccacaro, T., Della Cecca, R., Gioia, I. M., Morris, S. L., Stocke, J. T., & Wolter, A.
1991, *ApJ*, 374, 117
- Marshall, F. E., et al. 1993, *ApJ*, 405, 168
- Martel, A. R. 1997, *PASP*, 109, 630
- Miller, J. S., & Goodrich, R. W. 1990, *ApJ*, 355, 456
- Miller, J. S., & Stone, R. P. S. 1987, *Lick Obs. Tech. Rep.*, No. 48
- Moran, E., Halpern, J. P., Bothun, G. D., & Becker, R. H. 1992, *AJ*, 104, 990
- Mulchaey, J. S., Koratkar, A., Ward, M. J., Wilson, A. S., Whittle, M., Antonucci, R. J.
R., Kinney, A. L., & Hurt, T. 1994, *ApJ*, 436, 586
- Ogasaka, Y., Inoue, H., Brandt, W. N., Fabian, A. C., Kii, T., Nakagawa, T., Fujimoto, R.,
& Otani, C., 1997, *PASJ*, 49, 179
- Ohta, K., Yamada, T., Nakanishi, K., Ogasaka, Y., Kii, T., & Hayashida, K. 1996, *ApJ*,
458, L57
- Osterbrock, D. E., & Pogge, R. W. 1985, *ApJ*, 297, 166
- Puchnarewicz, E. M., et al. 1997, *MNRAS*, 291, 177
- Reynolds, C. S., Fabian, A. C., Makishima, K., Fukazawa, Y., & Tamura, T. 1994, *MNRAS*,
268, 55

- Salvati, M., Bassani, L., Della Ceca, R., Maiolino, R., Matt, G., & Zamorani, G. 1997 *A&A*, 323, L1
- Stark, A. A., Gammie, C. F., Wilson, R. W., Bally, J., Linke, R. A., Heiles, C. & Hurwitz, M. 1992, *ApJS*, 79, 77
- Steidel, C. C., & Sargent, W. L. W. 1991, *ApJ*, 382, 433
- Stephens, S. A. 1989, *AJ*, 97, 10
- Stocke, J., Liebert, J., Maccacaro, T., Griffiths, R. E., & Steiner, J. E. 1982, *ApJ*, 252, 69
- Stocke, J. T., Liebert, J., Gioia, I. M., Griffiths, R. E., Maccacaro, T., Danziger, I. J., Kunth, D., & Lub, J. 1983, *ApJ*, 273, 458
- Stocke, J. T., Morris, S. L., Gioia, I., Maccacaro, T., Schild, R. E., & Wolter, A., 1990, *ApJ*, 348, 141
- Tran, H. D., 1995, *ApJS*, 440, 565
- Turner, T. J., George, I. M., Nandra, K., & Mushotzky, R. F. 1997a, *ApJS*, 113, 23
- Turner, T. J., George, I. M., Nandra, K., & Mushotzky, R. F. 1997b, *ApJ*, 488, 164
- Ueno, S., Koyama, K., Nishida, N., Yamauchi, S., & Ward, M. J. 1994, *ApJ*, 431, L1
- Wills, B. J., & Hines, D. C. 1997, in *ASP Conf. Ser. 128, Mass Ejection from AGNs*, ed. N. Arav, I. Schlosman, & R. Weymann (San Francisco: ASP), 99
- Zheng, W., Kriss, G. A., Telfer, R. C., Grimes, J. P., & Davidsen, A. F. 1997, *ApJ*, 475, 469